In the format provided by the authors and unedited.

A potassium *tert*-butoxide and hydrosilane system for ultra-deep desulfurization of fuels

Anton A. Toutov,[1] Mike Salata,[2] Alexey Fedorov,[1,3] Yun-Fang Yang,[4] Yong Liang,[5] Renan Cariou,[2] Kerry N. Betz,[1] Erik P. A. Couzijn,[3] John W. Shabaker,[2] K. N. Houk[4] & Robert H. Grubbs[1]

john.shabaker@bp.com, houk@chem.ucla.edu, rhg@caltech.edu

[1]Division of Chemistry and Chemical Engineering, California Institute of Technology, Pasadena, California 91125, United States.
[2]BP Products North America, 150 West Warrenville Rd, Naperville, IL 60563.
[3]Department of Chemistry and Applied Biosciences, ETH Zürich, Vladimir-Prelog-Weg 2, CH-8093, Zürich, Switzerland.
[4]Department of Chemistry and Biochemistry, University of California, Los Angeles, California 90095, United States.
[5]State Key Laboratory of Coordination Chemistry, School of Chemistry and Chemical Engineering, Nanjing University, Nanjing, 210023, China.

Supplementary Note 1: Optimization of the hydrodesulfurization (HDS) of dibenzothiophene (1S).
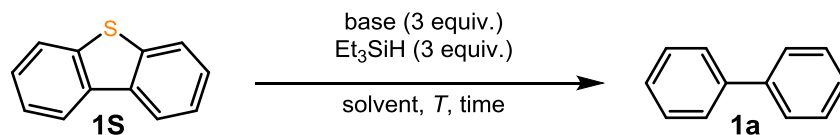
Investigating the HDS of dibenzothiophene under a variety of conditions revealed several important features of the reaction. First, the reaction appears to require a strong inorganic base (Supplementary Figure 1, entries 4–10). The reaction does not occur with potassium hydroxide (entry 3) or with organic bases (entries 11–13). Second, the use of a potassium base appears to be vital for HDS to occur; the reaction does not proceed with lithium- or sodium alkoxide bases (entries 1 & 2). Potassium *tert*-butoxide (KO*t*-Bu) proved to be the optimal base for the HDS (entry 7) as KOMe (entry 5) and KOEt (entry 6) afforded the product in significantly lower yield. It appeared then that the effectiveness of the *KO*R/*Si*-H (*KOSi*) system correlates with the basicity of the alkoxide; however, the ease of solubility of the base in the reaction medium cannot be discounted as a contributing factor. Third, the yield of biphenyl (**1a)** increases with increasing temperature (entries 7→10). Although considerations of energy input (especially on an industrial scale) led us to run the HDS reactions at 165 °C, it is gratifying to observe that increasing the temperature to 200 °C further improves the yield of **1a** (entry 10). Finally, triethylsilane (Et$_3$SiH) demonstrated the highest HDS activity; a dihydrosilane, Et$_2$SiH$_2$, performed poorly compared to Et$_3$SiH (entry 14). The light and low-boiling EtMe$_2$SiH was also less effective (entry 15).

No reaction occurs with Et$_4$Si (entry 16) clearly demonstrating, as anticipated, that a silane with an Si–H bond is required to induce HDS reactivity. A brief solvent investigation revealed that besides mesitylene, other simple aromatic (entries 18 & 21) as well as aliphatic (entry 19) hydrocarbons are superior solvents for this reaction, whereas ethers (entries 17 & 20) are poor or shut down reactivity (entry 23). Alcohols (entries 22 & 26), and amides (entries 24 & 25) likewise shut down the reactivity.

Supplementary Note 2: Robustness evaluation.

Practical considerations of the *KOSi* method will have an important impact on the likelihood of its eventual implementation in industry. Fortunately, a brief robustness evaluation demonstrates that the reaction is tolerant of conditions that model a general operating environment in a refinery setting (Supplementary Figure 2).

The robustness investigation conducted in the context of the *KOSi* HDS of 4,6-Me$_2$DBT (**3**) shows that the reaction tolerates impurities such as those that would be found in bulk, unpurified solvents and reagents and that it can be performed under air. A 10-hour reaction time leads to slightly lower conversion. The reaction shows some sensitivity to water, as would be expected given the sensitivity of KO*t*-Bu to moisture. Although impacting the yield (see **IV**), the reaction proceeds in the presence of ambient moisture both on the surface of the glassware as well as in the solvent and reagents. The reaction also proceeds well in ultra-low sulfur diesel (ULSD) as the solvent (see **V**).

The scalability of the reaction was also evaluated using dibenzothiophene (**1S**) due to its much lower cost and greater ease of synthesis compared to **3**. The reaction scales well with gram quantities of **1S** to give the hydrocarbon (**1a**) product in 53 % yield after 10 h at 165 °C.

Supplementary Note 3: Optimization of the *KOSi* HDS of 4,6-Me$_2$DBT in ULSD (3).

Having determined that the *KOSi* HDS of 4,6-Me$_2$DBT proceeds well in ULSD (Supplementary Figure 2, **V**) we proceeded to investigate the effect of various parameters on the reaction using ULSD as a practically-relevant model solvent. Decreasing the number of equivalents each of base and silane from 3 (Supplementary Figure 3, standard conditions; entry 1) to 2 (entry 2) to 1 (entry 3) shows a step-wise decrease of the yield. With 3 equivalents each of KO*t*-Bu and Et$_3$SiH the reaction time can be lowered to 10 hours with a slight drop in the yield (entry 4) as was shown in the case of mesitylene as the solvent (Supplementary Figure 2). Further lowering reaction time to 5 hours results in a large corresponding decrease in yield (entry 5). Et$_3$SiH could be replaced by polymethylhydrosiloxane (PMHS) – an inexpensive, non-toxic, air- and water stable polymeric hydrosiloxane which is a byproduct of the silicone industry – though with decreased yield.

In this latter case, despite the non-negligible decrease in yield, the fact that the *KOSi* reaction proceeds in the presence of such a simple, inexpensive, and abundantly available Si–H source is very surprising since PMHS is generally employed for facile reductions, most often of carbonyl derivatives. Most importantly, *KOSi* with PMHS is a vital proof of principle for future improvements toward eventual implementation.

Supplementary Note 4: Quantification of retained Si and K in the *KOSi* HDS of dibenzothiophene (1S).

The analysis demonstrated that the silicon remaining in the feed is very high. This is of course expected since the eventual fate of the Si atom is sequestration of the sulfur (see Figure 3A, **TS6_S** – formation of TMS_2S, and the discussion in the main text) and, like the potassium, no efforts were made to remove any of the silicon from the mixture so as not to affect the ultimate [S] quantification in any way. Any unreacted or oxidized silane will also remain in the feed due to low volatility. In order to advance the *KOSi* method from a decisive proof of principle to a practical polishing refining technology, the silicon source would have to be inexpensive such as PMHS (Supplementary Figure 3, entry 6). Conversely, homogeneous silicon species – such as those used and formed herein – could be removed from the feed by scrubbing or by distillation and ideally be reactivated and reused. Regarding the latter, since the major Si product is an Si–S–Si species, it may be possible to hydrogenate the two Si–S bonds using H_2 to reform the active hydrosilane (i.e., reform the Si–H bond) with concomitant release of H_2S. Work is currently ongoing toward this end.

Supplementary Note 5: Observation of deoxygenation of 4,6-dimethyldibenzofuran (3O) at high temperatures.

Having observed the efficient desulfurization activity of dibenzothiophene derivatives under the standard *KOSi* conditions, we became interested in whether O-heterocycles could potentially be deoxygenated as well. However, our earlier studies into reductive C–O cleavage emploing hydrosilane/base reductive systems showed no evidence of deoxygenation in dibenzofuran substrates such as **3O** and only single C–O bond cleavage was observed giving **3a–OH** (Supplementary Figure 5, entry 1).

At that point, it was not clear why deoxygenation in those substrates was not observed. However, with the knowledge gleaned from the density functional theory studies performed herein, it becomes clear that the barrier to deoxygenation of these substrates (e.g., **3O**) is simply too high to be overcome at the standard *KOSi* temperatures. Indeed, the energy for displacement of Me₃SiO by Me₃Si is quite high (37.5 kcal/mol). Increasing the temperature of the reaction to 165 °C (entry 2) and finally to 200 °C (entry 3) systematically results in increased conversions as expected and results in high yields of **3a–OH**. However, conducting the reaction at 200 °C for 60 h, 7% of **3a** is obtained, constituting the first observations of deoxygenation of a dibenzofuran derivative using the *KOSi* system. This result lends support to the proposed mechanism and correponding energetics provided by density functional theory calculations and warrants further exploration into hydrodeoxygenation (HDO) chemistry by *KOSi.*
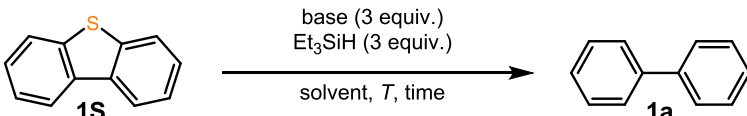
Supplementary Note 6: Free energies and transition states for the *KOSi* HDS of 4,6-dimethyldibenzothiophene (3).

Refer to Figure 3A in the main text. The carbon of the C–S bond of the substrate (**3**) is proposed to be attacked by silyl radical through **TS1_S** with a barrier of 15.5 kcal/mol to form **Int1_S**, which can undergo C–S bond homolytic cleavage through **TS2_S** (11.8 kcal/mol) to form **Int2_S**. The subsequent silyl radical migration from C to S through **TS3_S** has a high barrier of 31.8 kcal/mol. The direct attack onto the heteroatom, S, of the substrate was also considered, followed by C–S homolytic cleavage through **TS4_S**. This transition state has a lower barrier than the migration transition state **TS3_S** by 5.4 kcal/mol. Once the carbon radical species, **Int3_S**, is formed, it can abstract an H atom from trimethylsilane through **TS5_S** to form silylated biaryl-2-thiol **Int4_S**. This hydrogen abstraction step is the rate-determining step with an overall barrier of 27.2 kcal/mol. Then silyl radical attack at the S atom through **TS6_S** forms biaryl radical and disilathiane to complete the desulfurization process. Finally, the biaryl radical abstraction of an H atom from trimethylsilane (**TS7_S**) is a very facile process to generate the final biaryl product and regenerate the silyl radical. The overall process is exergonic by 32.7 kcal/mol. In summary, for substrate 4,6-dimethyldibenzothiophene (**3**), silyl radical attack at the heteroatom S and eventual attack of a second silyl radical at the S of the biaryl silyl thioether to give desulfurization is a favorable pathway. The calculated transition states discussed above are visualized in Supplementary Figure 6.

Supplementary Note 7: Free energies and transition states for the aryl C–O bond cleavage of 4,6-dimethyldibenzofuran (3O) by the *KOSi* method.

Refer to Figure 3B in the main text. Different from the 4,6-dimethyldibenzothiophene case (**3**), the direct attack of the silyl radical to the heteroatom of **3O**, breaking one C–O bond, is very unfavorable with a barrier of 43.3 kcal/mol (**TS4_O**). Instead, silyl radical attack at carbon atom of the C–O bond of 4,6-dimethyldibenzofuran (**3O**) through **TS1_O** has a barrier of 16.2 kcal/mol, leading to **Int1_O**, which undergoes C–O bond homolytic cleavage through **TS2_O** (22.4 kcal/mol) to generate **Int2_O**. The subsequent silyl radical migration from C to O through **TS3_O** requires an overall activation free energy of 26.7 kcal/mol and is the rate-determining step. The carbon radical species, **Int3_O**, is relative stable, and can abstract an H atom from trimethylsilane through **TS5_O** to form silylated biaryl-2-ol, **Int4_O**. The silyl radical reattacking the O atom through **TS6_O** is a very unfavorable process with a barrier of 37.5 kcal/mol. It is speculated that silylated biaryl-2-ol, **Int4_O**, can undergo hydrolysis to form the biaryl-2-ol product **3a–OH** that is observed experimentally. In summary, for substrate 4,6-dimethyldibenzofuran (**3O**), the silyl radical attack at O is unfavorable for both the substrate and the intermediate biaryl silyl ether. The silyl radical preferentially attacks the aryl group of the substrate and finally undergoes hydrolysis to generate biaryl-2-ol **3a–OH** instead of the deoxygenation product **3a**. The calculated transition states discussed above are visualized in Supplementary Figure 7.

Supplementary Figures

Supplementary Figure 1. Discovery and optimization of the *KOSi* HDS of dibenzothiophene (**1S**).

entry	base	[Si]–H	solvent	T (°C)	time (h)	yield 1a[a]
1	LiOt-Bu	Et$_3$SiH	Mesitylene	100	72	–
2	NaOt-Bu	Et$_3$SiH	Mesitylene	100	72	–
3	KOH	Et$_3$SiH	Mesitylene	100	72	–
4	KH	Et$_3$SiH	Mesitylene	100	40	12%
5	KOMe	Et$_3$SiH	Mesitylene	100	40	21%
6	KOEt	Et$_3$SiH	Mesitylene	100	40	29%
7	KOt-Bu	Et$_3$SiH	Mesitylene	100	40	46%
8	KOt-Bu	Et$_3$SiH	Mesitylene	120	40	66%
9	KOt-Bu	Et$_3$SiH	Mesitylene	165	40	83%
10	KOt-Bu	Et$_3$SiH	Mesitylene	200	40	90%
11	Pyridine	Et$_3$SiH	Mesitylene	165	72	–
12	DBU	Et$_3$SiH	Mesitylene	165	72	–
13	NEt$_3$	Et$_3$SiH	Mesitylene	165	72	–
14	KOt-Bu	Et$_2$SiH$_2$	Mesitylene	165	40	13%
15	KOt-Bu	EtMe$_2$SiH	Mesitylene	165	40	26%
16	KOt-Bu	Et$_4$Si	Mesitylene	165	72	–
17	KOt-Bu	Et$_3$SiH	THF	165	40	22%
18	KOt-Bu	Et$_3$SiH	Benzene	100	40	47%
19	KOt-Bu	Et$_3$SiH	MeCy	165	40	81%
20	KOt-Bu	Et$_3$SiH	1,4-dioxane	165	40	30%
21	KOt-Bu	Et$_3$SiH	Toluene	120	40	49%
22	KOt-Bu	Et$_3$SiH	t-BuOH	120	40	–
23	KOt-Bu	Et$_3$SiH	Diglyme	165	40	–
24	KOt-Bu	Et$_3$SiH	DMF	100	40	–
25	KOt-Bu	Et$_3$SiH	DMA	100	40	–
26	KOt-Bu	Et$_3$SiH	Diisopropyl carbinol	165	40	–

[a]Yields determined by GC-FID analysis using tridecane as a standard.

Supplementary Figure 2. Robustness evaluation of the *KOSi* HDS of 4,6-dimethyldibenzothiophene (**3**) and gram-scale HDS of dibenzothiophene (**1S**).
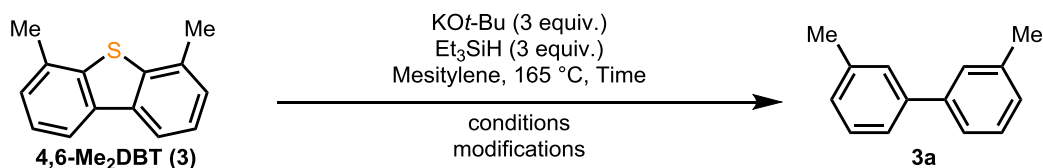
standard conditions: purified reagents, anydrous conditions, degassed liquids, nitrogen glovebox for 40 hours.

83% yield[a]

modifications:

I) Reaction set up and run outside the glovebox under nitrogen (simple air-free technique) for 40 hours. — 81%

II) I) + non-degassed solvent or silanes; reaction run for 10 hours. — 72%

III) II) + non-purified reagents and bulk screw-cap bottle solvent; no inert gas — 73%
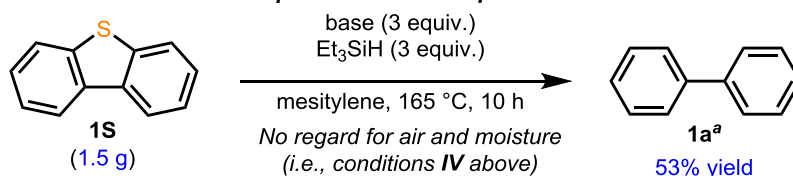
IV) III) + no regard for air and moisture (glassware off the rack, "dump and stir") — 42%

V) II) + ultra-low sulfur diesel (ULSD) as the solvent; reaction run for 40 hours. — 83%
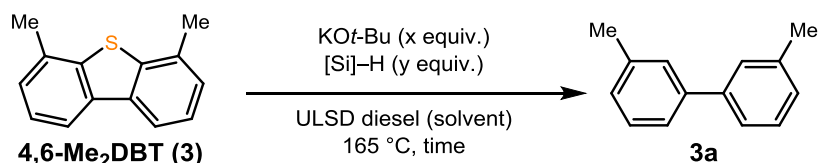
Gram-scale HDS of dibenzothiophene under "dump-and-stir" conditions

[a]Yields determined by GC-FID analysis using tridecane as a standard.

Supplementary Figure 3. *KOSi* HDS of 4,6-dimethyldibenzothiophene (**3**) under varying conditions.

entry	KOt-Bu (equiv.)	[Si]–H (equiv.)	time (h)	yield 3a[a]
1	3	Et$_3$SiH (3)	40	83%
2	2	Et$_3$SiH (2)	40	65%
3	1	Et$_3$SiH (1)	40	25%
4	3	Et$_3$SiH (3)	10	79%
5	3	Et$_3$SiH (3)	5	42%
6	3	PMHS (3)	40	49%

[a]Yields are by GC-FID analysis using tridecane as a standard.

Supplementary Figure 4. Evaluation of Si and K content remaining in the feed after *KOSi* HDS.

Feed: 1s in mesitylene
Si content in feed (ppm): 5772
K content in feed (ppm): 657
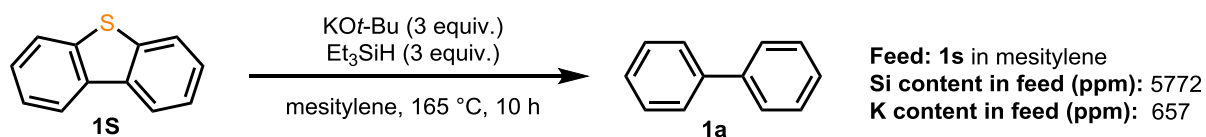
Supplementary Figure 5. Observed deoxygenation of 4,6-dimethyldibenzofuran (**3O**).
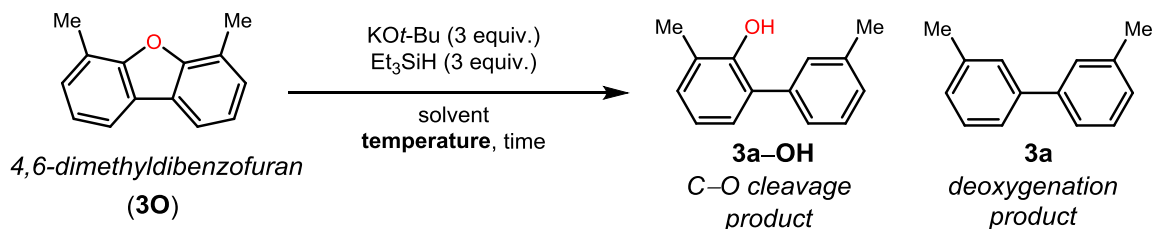
entry	solvent	temperature (°C)	time (h)	yield 3a–OH[a]	yield 3a[a]
1	toluene	100	20	78%	–
2	mesitylene	165	20	96%	–
3	mesitylene	200	60	93%	7%

[a]Yields are by GC-FID analysis with tridecane as a standard.

Supplementary Figure 6. Key transition states for *KOSi* HDS of 4,6-dimethyldibenzothiophene (**3**).
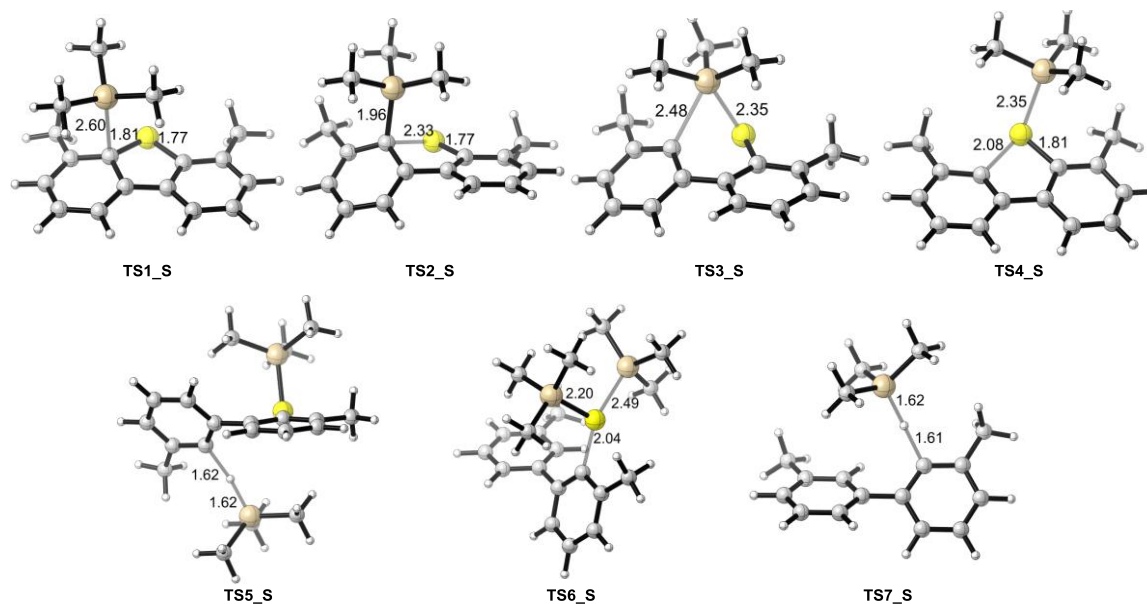
Supplementary Figure 7. Key transition states for reductive C–O bond cleavage in 4,6-dimethyldibenzofuran (**3**) by the *KOSi* method.
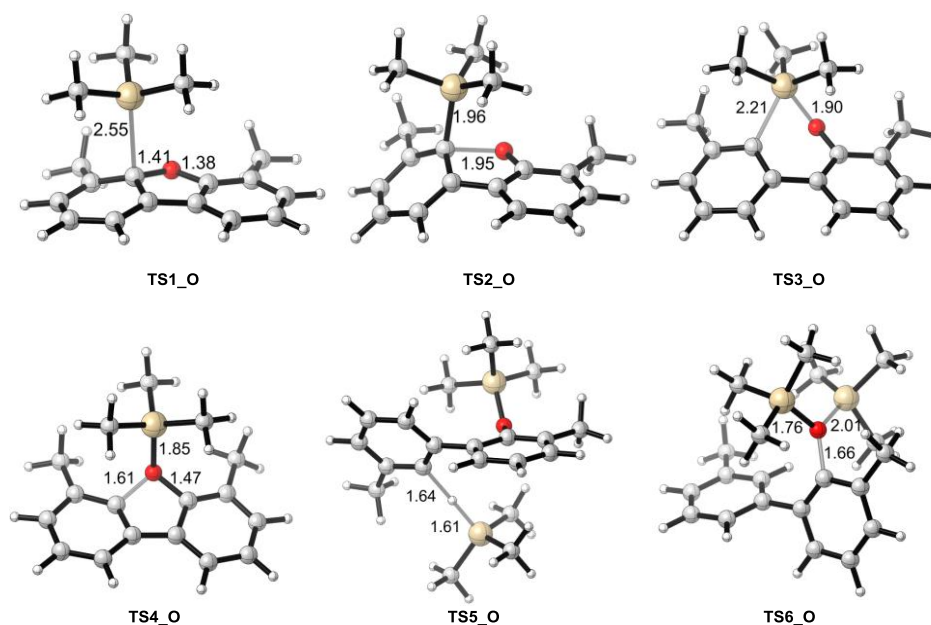
Supplementary Tables

Supplementary Table 1. Electronic energies, enthalpies, and free energies of the structures calculated at the M06-2X/6-311+G(d,p) (CPCM^{mesitylene})//B3LYP/ 6-31G(d).

Structures	ZPVE	TCE	TCH	TCG	Esol	Hsol (Esol + TCH)	Gsol (Esol + TCG)	Imaginary Frequency (cm^{-1})	ΔEsol (kcal/mol)	ΔHsol (kcal/mol)	ΔGsol (kcal/mol)
·SiMe₃	0.110424	0.117885	0.118829	0.079221	-409.158357	-409.039528	-409.079136	—	—	—	—
3	0.217085	0.229713	0.230657	0.178435	-938.839221	-938.608564	-938.660786	—	0.0	0.0	0.0
Int1_S	0.328288	0.349215	0.350159	0.279833	-1348.014038	-1347.663879	-1347.734205	—	-10.3	-9.9	3.6
Int2_S	0.330154	0.351135	0.352080	0.280549	-1348.012083	-1347.660003	-1347.731534	—	-9.1	-7.5	5.3
Int3_S	0.328484	0.350246	0.351190	0.276754	-1347.992661	-1347.641471	-1347.715907	—	3.1	4.2	15.1
Int4_S	0.341170	0.363113	0.364057	0.289086	-1348.674759	-1348.310702	-1348.385673	—	-17.4	-14.2	-4.1
Int5_S	0.224008	0.236741	0.237686	0.181958	-541.146777	-540.909091	-540.964819	—	-24.5	-21.6	-12.8
3a	0.237022	0.249704	0.250648	0.196045	-541.831749	-541.581101	-541.635704	—	-46.9	-41.7	-32.7
TS1_S	0.327127	0.348360	0.349304	0.276936	-1347.992210	-1347.642906	-1347.715274	-337.565	3.4	3.3	15.5
TS2_S	0.328544	0.348977	0.349922	0.280571	-1348.001678	-1347.651756	-1347.721107	-120.53	-2.6	-2.3	11.8
TS3_S	0.328904	0.349338	0.350282	0.280941	-1347.970110	-1347.619828	-1347.689169	-202.426	17.2	17.7	31.8
TS4_S	0.327483	0.348823	0.349767	0.276719	-1347.974625	-1347.624858	-1347.697906	-246.532	14.4	14.6	26.4
TS5_S	0.445642	0.476409	0.477353	0.381812	-1757.796673	-1757.319320	-1757.414861	-837.468	5.4	5.2	27.2
TS6_S	0.451190	0.482019	0.482964	0.386782	-1757.827069	-1757.344105	-1757.440287	-270.192	-13.6	-10.3	11.3
TS7_S	0.341541	0.363019	0.363963	0.288859	-950.953069	-950.589106	-950.664210	-837.588	-23.6	-21.9	-0.9
3O	0.220027	0.232261	0.233205	0.181464	-615.861082	-615.627877	-615.679618	—	0.0	0.0	0.0
Int1_O	0.331020	0.351420	0.352365	0.283120	-1025.031234	-1024.678869	-1024.748114	—	-7.4	-7.2	6.7
Int2_O	0.331018	0.352039	0.352984	0.281176	-1025.038304	-1024.685320	-1024.757128	—	-11.8	-11.2	1.0
Int3_O	0.330414	0.351891	0.352836	0.278016	-1025.041895	-1024.689059	-1024.763879	—	-14.1	-13.6	-3.2
Int4_O	0.343489	0.364900	0.365844	0.292144	-1025.726940	-1025.361096	-1025.434796	—	-36.5	-33.7	-23.1
TS1_O	0.330084	0.350780	0.351724	0.280156	-1025.013163	-1024.661439	-1024.733007	-339.657	3.9	3.7	16.2
TS2_O	0.330092	0.350194	0.351138	0.282888	-1025.005890	-1024.654752	-1024.723002	-254.07	8.5	7.9	22.4
TS3_O	0.330244	0.350341	0.351285	0.282306	-1024.998477	-1024.647192	-1024.716171	-183.413	13.2	12.7	26.7
TS4_O	0.327728	0.348515	0.349459	0.278658	-1024.968347	-1024.618888	-1024.689689	-642.444	32.1	30.4	43.3
TS5_O	0.447660	0.478053	0.478997	0.384030	-1434.848709	-1434.369712	-1434.464679	-703.013	-13.5	-14.3	7.8
TS6_O	0.452636	0.482724	0.483668	0.391004	-1434.845160	-1434.361492	-1434.454156	-765.371	-11.3	-9.1	14.4
·SiEt₃	0.197772	0.209068	0.210012	0.159653	-527.056709	-526.846697	-526.897056	—	—	—	—
TS1_S_Et	0.414615	0.439549	0.440493	0.359844	-1465.890237	-1465.449744	-1465.530393	-346.000	3.6	3.5	17.2
TS4_S_Et	0.414891	0.440035	0.440980	0.358859	-1465.875045	-1465.434065	-1465.516186	-253.873	13.1	13.3	26.1

ZPVE = zero-point vibrational energy; **TCE** = thermal correction to energy; **TCH** = thermal correction to enthalpy;
TCG = thermal correction to Gibbs free energy.